

Satellite Laser Ranging System at Geochang Station

Hyung-Chul Lim^{1†}, Ki-Pyoung Sung¹, Sung-Yeol Yu¹, Mansoo Choi¹, Eunseo Park¹,
Jong-Uk Park¹, Chul-Sung Choi¹, Simon Kim^{1,2}

¹Korea Astronomy and Space Science Institute, Daejeon 34055, Korea

²University of Science and Technology, Daejeon 34113, Korea

Korea Astronomy and Space Science Institute (KASI) has been developing the space optical and laser tracking (SOLT) system for space geodesy, space situational awareness, and Korean space missions. The SOLT system comprises satellite laser ranging (SLR), adaptive optics (AO), and debris laser tracking (DLT) systems, which share numerous subsystems, such as an optical telescope and tracking mount. It is designed to be capable of laser ranging up to geosynchronous Earth orbit satellites with a laser retro-reflector array, space objects imaging brighter than magnitude 10, and laser tracking low Earth orbit space debris of uncooperative targets. For the realization of multiple functions in a novel configuration, the SOLT system employs a switching mirror that is installed inside the telescope pedestal and feeds the beam path to each system. The SLR and AO systems have already been established at the Geochang station, whereas the DLT system is currently under development and the AO system is being prepared for testing. In this study, the design and development of the SOLT system are addressed and the SLR data quality is evaluated compared to the International Laser Ranging Service (ILRS) tracking stations in terms of single-shot ranging precision. The analysis results indicate that the SLR system has a good ranging performance, to a few millimeters precision. Therefore, it is expected that the SLR system will not only play an important role as a member of the ILRS tracking network, but also contribute to future Korean space missions.

Keywords: nanosatellite, power budget, energy balance analysis, graphic user interface

1. INTRODUCTION

Satellite laser ranging (SLR) provides the distance to Earth orbit satellites with a laser retro-reflector array (LRA) using ultra-shot pulse lasers, which has been known to be the most precise range measurement technique, with millimeter precision. It has been used for geodesy, geophysics, and fundamental research as well as precise orbit determination (POD) because of the capability of measuring ranges of normal point data with millimeter precision (Lim et al. 2011). Therefore, the SLR technology provides a powerful tool to independently validate the satellite orbits of global navigation satellite system (GNSS) derived using microwave measurements (Urschl et al. 2005). Recently, numerous countries have launched global navigation satellites with an LRA to establish new regional or global satellite navigation system (ILRS 2018), such as the European Galileo, Chinese Beidou, Japanese quasi-zenith satellite system

(QZSS), and Indian regional navigation satellite system (IRNSS). In the case of the Beidou, QZSS, and IRNSS systems, numerous satellites are located in geosynchronous Earth orbit (GEO), whereas all the Galileo satellites are in medium Earth orbit. Therefore, the international demand for establishing additional SLR systems is gradually increasing to track the GNSS satellites, even though there are already approximately 50 SLR stations in 25 countries.

It is known that Korea has a plan to launch navigation satellites with LRAs, and will launch a GEO satellite, called GEO-KOMPSAT-2B with an LRA comprising 84 corner cubes, for remote sensing in 2019. The circular GEO satellite will be required to perform periodic station-keeping maneuvers because of a number of perturbations that cause orbit inclination, longitude, and eccentricity to drift over time. The frequent station-keeping maneuvers resulting from inaccurate POD based on microwave measurements reduce the satellite

© This is an Open Access article distributed under the terms of the Creative Commons Attribution Non-Commercial License (<https://creativecommons.org/licenses/by-nc/3.0/>) which permits unrestricted non-commercial use, distribution, and reproduction in any medium, provided the original work is properly cited.

Received 19 OCT 2018 Revised 7 DEC 2018 Accepted 8 DEC 2018

[†]Corresponding Author

Tel: +82-42-865-3235, E-mail: hclim@kasi.re.kr

ORCID: <https://orcid.org/0000-0001-5266-1335>

lifetime because of fuel consumption when maintaining the desired orbital positioning. However, the GEO POD using SLR measurements, obtained from a stand-alone station, gives a more accurate POD than microwave measurements if the SLR measurements are provided continuously over a specific period (Oh et al. 2017). Therefore, these satellites require an SLR station in Korea to track the GEO satellites.

Recently, space debris has become a critical issue as the amount of debris is increasing rapidly, specifically in the low Earth orbit (LEO) region between 700 and 1,000 km. It is predicted that a collisional cascade, known as the Kessler syndrome (Kessler & Cour-Palais 1978), will occur if action is not taken to reduce the amount of space debris, such as collision avoidance and mitigation (Liou 2013). The present catalog of two-line elements (TLE) is maintained based on radar and passive optical tracking data, which does not provide the required orbit accuracy for the space debris collision warnings in space situational awareness (SSA). Therefore, more accurate orbital prediction (OP) of space debris is required to avoid catastrophic space disasters of space debris collision against operating satellites or the international space station. The ground-based laser has been recognized as an additional tool to create a more accurate catalog of space objects, including satellites and space debris and, therefore, numerous SLR stations have developed laser ranging technologies for space debris, which is known as uncooperative targets (Greene et al. 2002; Zhang et al. 2012; Kirchner et al. 2013; Lejba et al. 2018). Current laser ranging precision to space debris is achievable in the range of 50-250 cm, one or two orders of magnitude better than radar and passive optical tracking systems. In addition, good OP accuracy of space objects is available from the combination of laser ranging and passive optical tracking data, which is obtained even from a single station (Bennett et al. 2015).

Adaptive optics (AO) has been utilized in astronomical and military applications because of its ability to compensate for phase distortions of light waves in real time. In addition, it has attracted attention since 2000 in two SSA categories: space object imaging and space debris removal based on the ground-based high-power laser (Mason et al. 2011; Bennet et al. 2016; Zovaro et al. 2016; Grosse et al. 2017). To improve the OP precision of space objects, the advanced model should consider not only the ranging measurement, but also the shape, structure, and orientation information available from the characterization and identification based on the AO high-resolution imagery. When a laser propagates through the atmosphere, it suffers from the detrimental effects of atmospheric turbulence that results in the focused spot in space being broadened and distorted (Gebhardt 1976). However, the AO compensates for atmospheric turbulence

and then allows the high-power laser to ablate or vaporize the space debris.

Korea Astronomy and Space science Institute (KASI) has operated the SLR system at the Sejong station since 2017 for space geodesy and spin dynamics research (Choi et al. 2014; Choi et al. 2015), and has been also developing the space optical laser tracking (SOLT) system at the Geochang station for space geodesy, SSA and Korean space missions. The SOLT system consists of the SLR, AO and debris laser tracking (DLT) systems which are composed of a dedicated module and a common module. The three systems are operated independently but not simultaneously by rotating the switching mirror inside the telescope pedestal which feeds the beam path to each system. The SLR and AO systems have been established at the Geochang station whereas the DLT system is currently under development. The SOLT system has a novel, effective and cost-optimized configuration in order to execute three independent systems. Especially the SLR system will participate in the International Laser Ranging Service (ILRS) tracking network after its ranging performance is evaluated. In this study, we address the design and development of the SOLT system and the SLR system performance is evaluated compared with those of the ILRS tracking stations in terms of single-shot ranging precision. It is demonstrated that the SLR system is capable of laser ranging up to GEO satellites with LRAs and shows a good ranging performance to a few millimeters precision. Thus it is expected that the SLR system will not only play an important role as a member of the ILRS tracking network, but also contribute to future Korean space missions.

2. SOLT SYSTEM

As can be seen in Fig. 1, the SOLT system comprises the SLR, AO, and DLT systems that include a common module and a

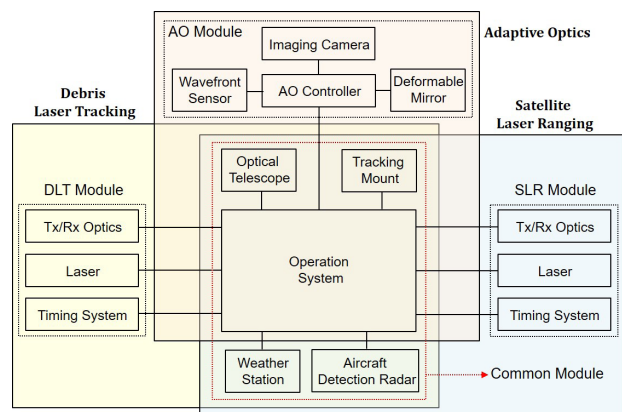


Fig. 1. Configuration of SOLT system.

dedicated module (SLR, AO, or DLT module). The SLR module was developed in collaboration with EOS Space Systems Ltd. in Australia, and the AO module with the Australian National University. The SLR system has two categories in terms of the optical path: monostatic (or common Coudé) system, and bistatic system. The monostatic system adopts one optical telescope for transmitting and receiving optical beams, whereas the bistatic system uses two telescopes. The SOLT system has a monostatic optical path and, therefore, the Coudé path terminates at the switching mirror in the telescope pedestal that can direct the optical beam to one of three modules installed in each Coudé laboratory

2.1 Common Module

The common module comprises an optical telescope, tracking mount, weather station, aircraft detection radar, and operating system. The optical telescope is designed as a confocal paraboloid beam expander configuration with a 100 cm clear aperture primary mirror (M1) having a focal ratio of $f/1.5$. The M1 support design is a passive 9-point axial whiffletree, and the lateral support system utilizes the central hole in the mirror using an Invar flexural system. The telescope focus is automatically controlled with 10 μm accuracy against the thermal expansion of telescope based on the temperature measurement of the optical tube assembly (OTA) and compensation by the primary/secondary mirror spacing. Pointing and wavefront errors because of thermal and gravitational effects are dynamically corrected within the optical error budget. Over the elevation range of 15° – 90° these errors are less than 0.3 arcsec and 100 nm, respectively. The SOLT system has seven Coudé mirrors (or switching mirrors), M1 to M7, to feed the optical beam to the SLR, AO, or DLT module, which are all coated against a high-power laser for DLT operation.

The tracking mount has a large hollow shaft for the optical beam path of 300 mm diameter, which is of the alt-azimuth type. It is required to be controlled fast and accurately to track LEO space debris, even at an altitude of 200 km. To realize this requirement, two arc motors with a maximum torque of 3,900 Nm for azimuth and 1,068 Nm for elevation were specifically developed and implemented. The stability of the telescope invariant point is critical for accurate ranging to satellites, and is located at the intersection of the elevation and OTA optical axes. Therefore, the tracking mount is designed and manufactured to maintain the invariant point within a 500 μm intersection error and 5 arcsec orthogonality.

The SOLT system operates two devices to detect an aircraft: aircraft detection radar and IR camera. The aircraft detection radar provides a means of detecting an aircraft before it

intersects a transmitted laser beam, and provides a signal to disable the laser fire automatically in the case of aircraft detection. This function is achieved by the use of a pedestal-mounted radar that is slaved and boresighted to the optical telescope. When the IR camera on the OTA detects an aircraft, it also sends an interlock command to the interlock server to disable the laser fire. The laser fire is paused in the laser oscillator when either the aircraft detection radar or the IR camera detects an aircraft, which will increase system reliability even though they frequently recognize heavy cloud as an aircraft.

The operating system is designed based on a client-server architecture on which commands and status responses are available over the network. Fig. 2 shows the software architecture for the SLR and DLT system operation, where the number is the task sequence. The satellite imaging camera and AO servers are added in the software architecture for the AO system operation. The predicted orbit of space objects is computed from TLE or consolidated prediction format ephemeris and the tracking schedule is then generated. The SLR system is operated manually or automatically, from either the local site or remote-control site, whereas the AO and DLT systems are operated only in the manual mode. Table 1 presents the specifications of the SOLT system according to the SLR, AO, DLT, and common modules.

2.2 SLR Module

The SLR module comprises a laser, Tx/Rx optics, and a timing system. The SLR laser is based on a mode-locked Nd:YAG laser system, which has a primary wavelength of 1,064 nm and a secondary wavelength of 532 nm converted by a second harmonic generator for satellite ranging. The SLR laser operates one of two modes: reduced mode, or full power mode. A diode-pumped passively mode-locked laser oscillator and a diode-pumped regenerative amplifier operate only in the reduced power mode. This mode is activated for ground target ranging and optical alignment because the pulse energy is controlled to a μJ level, which is eye-safe according to laser safety standards. In the full power mode, a diode-pumped power amplifier operates in addition to the diode-pumped oscillator and regenerative amplifier, producing pulse energies up to 15 mJ at 532 nm. When operated in the full power mode, the laser system is subject to a number of laser interlocks, such that if any interlock is activated, then laser emission is inhibited. The source of these interlocks may be physical (system failure, weather, or misalignment between telescope and dome positions) or scheduled because of restrictions on tracking certain satellites.

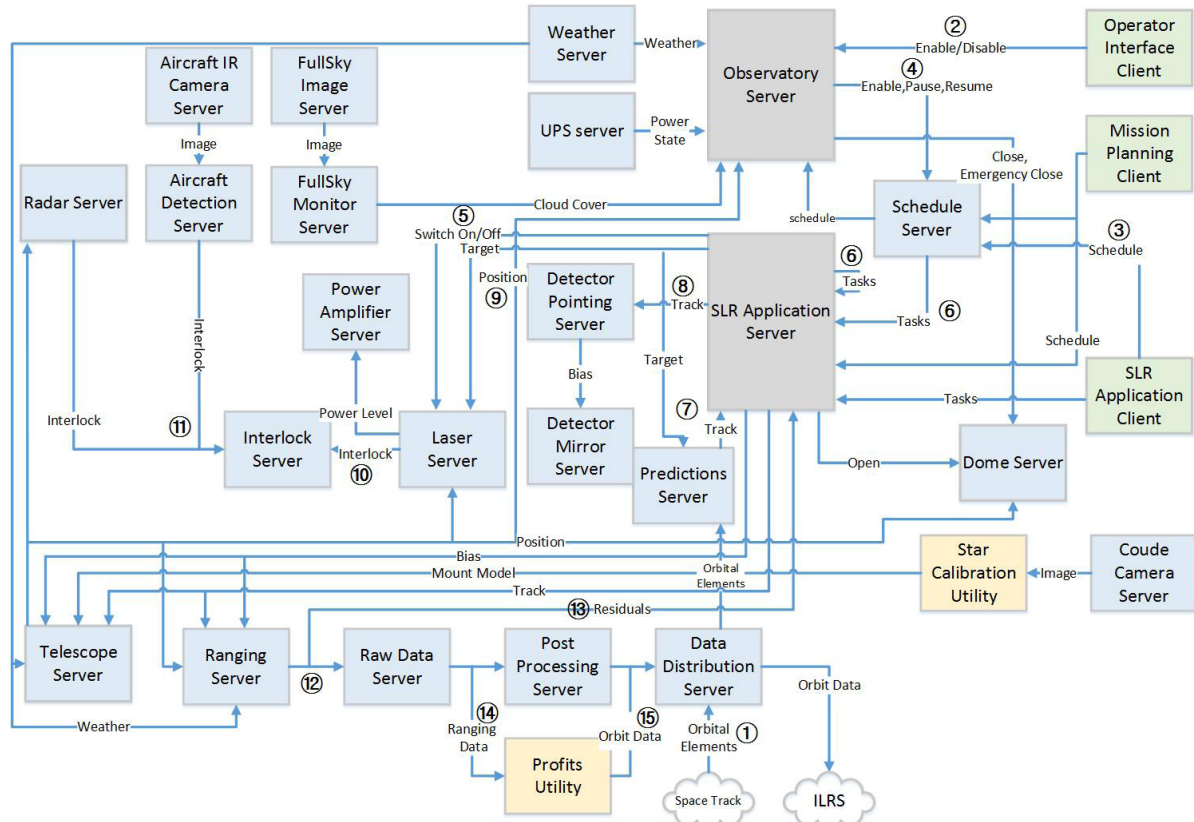


Fig. 2. Software architecture of operation system.

Table 1. Specifications of SOLT system

Module	Parameter	Value
Common	Optical path type	Common coude
	Primary mirror clear aperture	1,000 mm
	Secondary mirror clear aperture	250 mm
	Primary mirror F-ratio	1.5
	Mount slew rate (Az, El)	30 deg/s, 15 deg/s
	Mount acceleration (Az, El)	10 deg/s ² , 5 deg/s ²
	Tracking & pointing accuracy	1 arcsec
SLR	Laser wavelength	532 nm
	Laser pulse energy	15 mJ
	Laser pulse width	9.2 ps
	Laser repetition rate	60 Hz
	Detector quantum efficiency	20 % @ 532 nm
	Spectral filter bandwidth	2 nm @ 532 nm
	Spectral filter transmission	90 %
AO	Deformable mirror channel	97
	Deformable mirror operation rate	≤ 2 kHz
	Wavefront sensor subaperture	88
	Wavefront sensor wavelength	450 - 800 nm
	Wavefront sensor rate	≤ 2 kHz
	Imaging camera wavelength	800 - 1,000 nm
	Correction rate	≤ 2 kHz
DLT	Laser wavelength	532 nm
	Laser pulse energy	2.5 J
	Laser pulse width	4 - 8 ns
	Laser repetition rate	10 Hz
	Detector quantum efficiency	> 60 % @ 532 nm
	Spectral filter bandwidth	2.2 nm @ 532 nm
	Spectral filter transmission	> 90 %

The SLR Tx/Rx optics comprises a receiving box, T/R disk, beam expander, and Coudé camera. There are three types of filters (neutral density, spatial, and spectral filters), a spinning shutter, a compensated-single photon avalanche diode (C-SPAD) detector, and a charge-coupled device (CCD) camera inside the receiving box. The CCD camera is used for the optical alignment, whereas the Coudé camera is used for star calibration to estimate 35 parameters of the mount model to achieve the requirement of tracking and pointing accuracy. The spinning T/R disk has two clear apertures with a 30 mm diameter, allowing transmission of the laser beam, and one reflective surface that directs returned photons to the C-SPAD detector. The operating system controls the frequency of the T/R disk and adjusts it in real time to preclude returned photons coinciding with new laser pulses. It precomputes these collision bands and adjusts the spinning rate by up to 10 % . The laser beam is magnified by two beam expanders (x3.2 and x7) and the telescope (x4), resulting in an 896 mm diameter at the exit of telescope. The C-SPAD detector with single photon sensitivity and millimeter bias under controlled conditions has a small active area with a 0.2 mm diameter, which is sufficient to provide a field-of-view of 20 arcsec .

As can be seen in Fig. 3, the SLR timing system comprises a GPS receiver, event generator, event timer, delay generator,

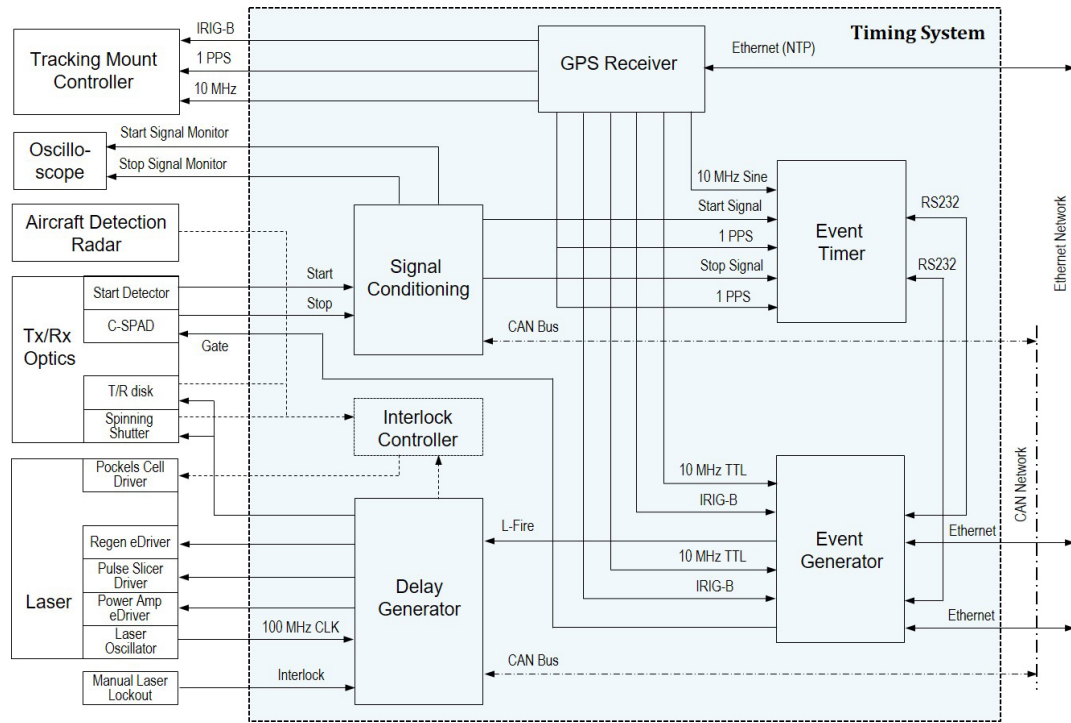


Fig. 3. Block diagram of SLR timing system.

signal conditioning, and an interlock controller. The event generator generates the laser fire command, L-Fire, and range gate signal with a 100 ns resolution at the epoch provided by the operating system, which is synchronized to the GPS timing using 10 MHz TTL (transistor-transistor logic) and IRIG-B signals. The delay generator receives the laser fire command from the event generator, and then produces a series of output pulses used to synchronize the T/R disk and the spinning shutter and trigger the generation of laser pulses. It is also synchronized to the laser oscillator providing 100 MHz clock signals to match the speed of the T/R disk and the spinning shutter with laser firing. The interlock controller monitors the interlock inputs of the TTL signals from the spinning shutter, T/R disk, and aircraft detection radar, and then sends an actual laser inhibit signal to the Pockels cell driver in the case of TTL signal detection of a 0 V level. The electrical signals from both the start detector and the C-SPAD are transferred to the event timer after being transformed into signal types, by signal conditioning, for the event timer and oscilloscope inputs. The event timer measures the event epochs of the start and stop signals accurately based on 1 pulse per second synchronized pulses and 10 MHz reference frequency from the GPS time frequency receiver. It provides sub-picosecond timing resolution (<0.9 ps RMS), long term stability (<25 fs/h), and non-linearity (<300 fs RMS) as well as being completely self-calibrating.

2.3 AO Module

AO is a technology to improve the performance of optical systems by reducing the effects of atmospheric distortion by measuring a distorted wavefront and then controlling a deformable mirror (DM) to compensate for the distortion. The AO system is designed to image space objects brighter than magnitude 10 up to an altitude of 1,000 km, and achieve a Strehl ratio greater than 20 % in an environment with good visibility with a Fried parameter of 12-15 cm. It uses the space object as a wavefront reference source of light, called a guide star, to measure a distorted wavefront because of atmospheric turbulence.

As can be seen in Fig. 4, the AO optical module comprises a wavefront sensor (WFS), DM, and imaging camera, which is installed on the optical bench in a clean and temperature controlled Coudé laboratory. The collimated beam from the telescope via the Coudé path is reduced by a beam expander, from 250 mm to 12.5 mm in beam diameter, and passed on to the DM in which the incoming wavefront is corrected. The DM, which has 97 actuators specified to operate up to 2 kHz with a 30 μ m full stroke, provides tip-tilt correction without a high-order correction device. The dichroic beamsplitter splits optical beams by wavelength, with 400-800 nm passing through to the WFS and 800-1,000 nm reflected to the imaging camera. The WFS is a Shack-Hartmann sensor to measure wavefront slopes, and

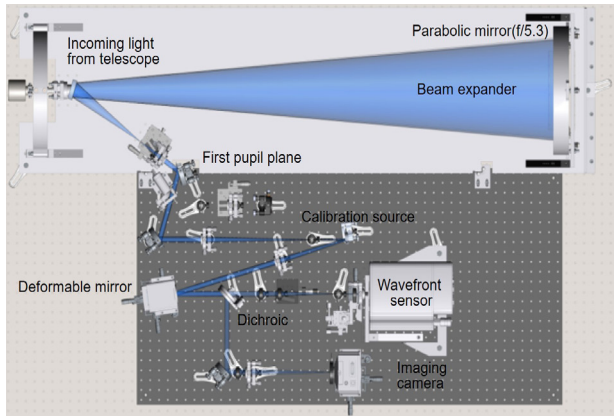


Fig. 4. Optical schematic of AO module.

comprises a lenslet array producing 8×8 subapertures and an electron-multiplying CCD (EMCCD) camera operating up to 2 kHz with extremely low readout noise (< 0.3 e⁻). The WFS also has a beam expander converting the beam from 12.5 mm to 2.5 mm. The beam expander comprises three lenses, the first two forming a compound lens to adjust the precise size of the beam. The pupil is also relayed, making the DM conjugate to the microlens array. The microlens array has a pitch of 300 μm and a radius of curvature of 9.5 mm, which achieves a pixel scale of 0.596 arcsec per pixel. The EMCCD camera is cooled to -40°C with liquid cooling and a thermoelectric cooler because it could be damaged by over illumination while the electron-multiplying gain is greater than 1. The imaging camera using the EMCCD operates at up to 60 Hz, and the imaging data is processed using a shift-and-stack algorithm in real time to remove the need for derotating optics or large stroke tip-tilt correction.

The AO control system transforms the measurements from a WFS into a sequence of control signals to control the shape of a DM in real time. For real time control, it has a Linux-based platform using C/C++ and PCIe cards that provide interfaces to the WFS and the DM. This architecture and specialized controller allow the AO system to achieve a closed loop rate up to 2 kHz.

2.4 DLT Module

The combination of optical and laser ranging data obtained from even a single station improves the OD of space debris throughout the estimation of an accurate ballistic coefficient (Bennett et al. 2015). Therefore, the DLT system is designed to provide angular measurements as well as range data of space debris because of the high tracking accuracy of the telescope, which is currently under development. The principle of range measurement is similar to the SLR system;

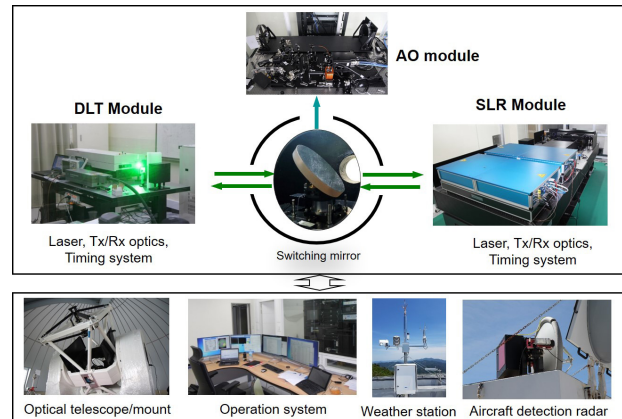


Fig. 5. SOLT system established at Geochang station.

however, the angular measurements are different from those of active optical tracking (Hampf et al. 2014) because the measurements come from the encoder values of the tracking mount and the pixel position of an array detector sensing the returned photons from space debris. The detector pixel may be triggered either by signals and noises from the background and dark current or not at all. When triggered by noises, these measurements are removed by applying the statistical signal processing that has been used to generate full rate data or normal point in the consolidated range data format (ILRS 2018). The triggered and filtered pixel provides range and angular information simultaneously, as opposed to active or passive optical tracking which extracts the angular data including right ascension and declination by comparison with the well-known star catalog. Unlike the active optical tracking requiring a high-power laser to illuminate space debris, this method provides the angular information in the environment of a very low signal-to-noise ratio environment resulting from a low power laser.

Fig. 5 shows the SOLT system established at the Geochang observatory, which is located 950 m above sea level to improve the image quality of space objects from the AO system.

3. SLR OBSERVATIONS AND ANALYSIS

The SLR system is currently under test and the AO system is being prepared for testing. Therefore, a number of representative observations to validate the SLR performance are discussed and analyzed in this section. Typically, the SLR data quality is evaluated in terms of single-shot precision for the ground target and satellites equipped with LRAs. The ground target laser ranging is conducted to estimate the system delay, including cable delay, optical path, and signal processing time, which allows an accurate determination of the distance

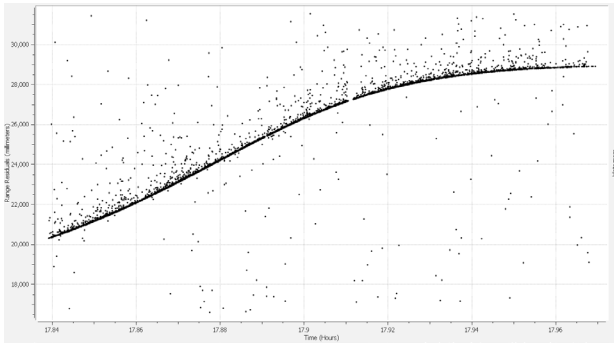


Fig. 6. Starlette observation results (August 2, 2018).

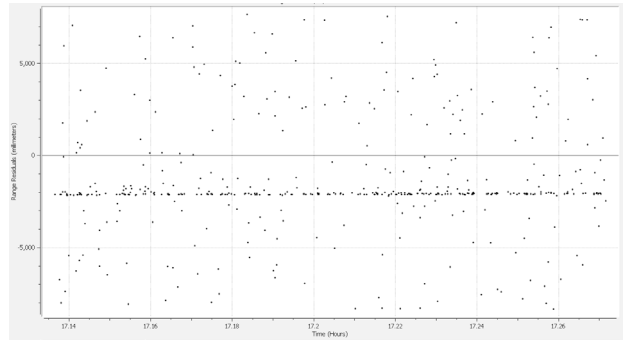


Fig. 9. Galileo 104 observation results (August 3, 2018).

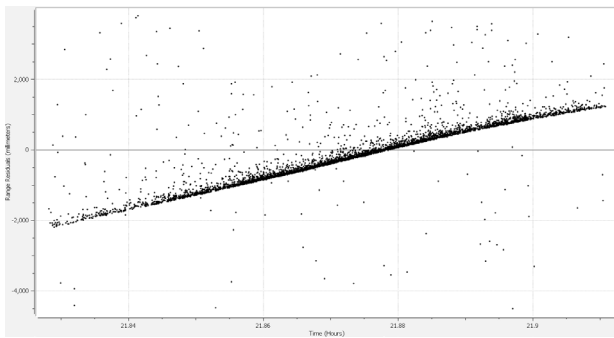


Fig. 7. Ajisai observation results (August 3, 2018).

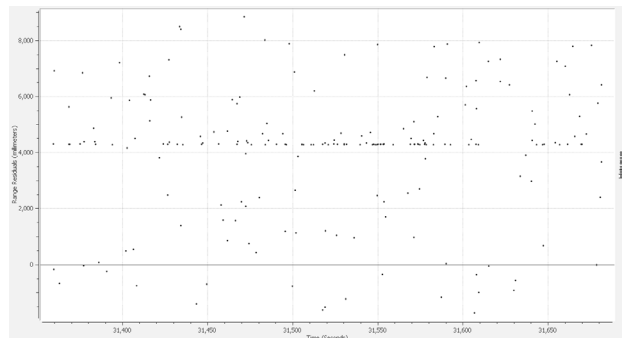


Fig. 10. Compass-G1 observation results (October 8, 2018).

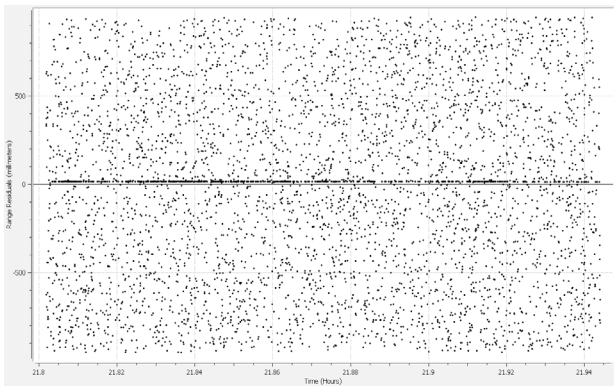


Fig. 8. Lageos-2 observation results (August 2, 2018).

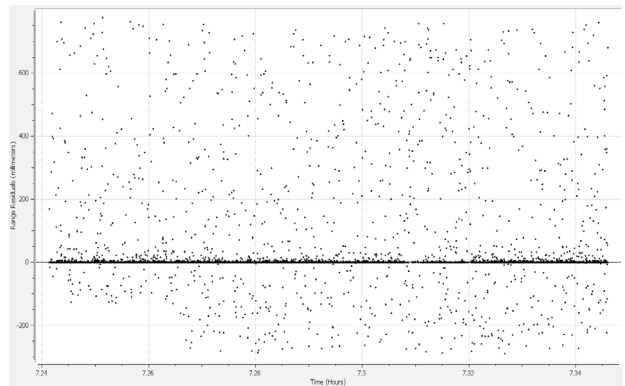


Fig. 11. Ground target observation results (August 3, 2018).

from the satellites to the telescope invariant point.

The SLR observations are shown in Figs. 6-11 for the five satellites, Starlette, Ajisai, Lageos-2, Galileo 104, and Compass-G1, as well as the ground target. These graphs show the ranging residuals (measured ranges minus predicted values) of single-shot with respect to the observation time. Table 2 presents the specifications and SLR data quality for the laser ranging targets. The average number of photons received at the detector depends on distance to the satellite, LRA characteristics, atmospheric attenuation, and system specifications. On the other hand, the SLR data quality is dominated significantly by the LRA characteristics and system performance, such as laser pulse width and timing

accuracy. As shown in Table 2, the single-shot precision of Ajisai satellite is larger than other ranging targets due to the LRA characteristics of large spherical shape with 215 cm diameter. Fig. 10 shows that the Geochang SLR system is capable of tracking the GEO satellites even though the amount of received photons is less than that from the other satellites. However, the received photons from the GEO satellites are expected to increase through fine alignment using stellar light at the C-SPAD detector.

The single-shot precision is calculated by the normal point algorithm (ILRS 2018) based on the statistical signal processing to remove outliers and noises from raw measurements, which means the RMS of fitting residuals for remaining

Table 2. Specifications and SLR data quality for laser ranging targets

Target	Mission	# of retro-reflector	Altitude (km)	Single-shot precision(mm)
Starlette	Gravity field	60	815	5.3
Ajisai	Geodesy	1,436	1,485	20.0
Lageos-2	Geodesy	426	5,625	7.1
Galileo 104	Positioning	84	23,220	13.2
Compassg1	Positioning	901	35,786	9.4
Ground target	Calibration	1	37 m (distance)	3.6

measurements after the signal processing. In the case of the ILRS tracking network, the SLR system performance is evaluated by single-shot precision for three ranging targets: Starlette, Lageos, and ground target. The ILRS publishes a monthly global report card including the average single-shot precision of these ranging targets during the previous 12 months for all the ILRS tracking stations (ILRS 2018). The recent report card for September 2018, states that the average precision is 9.7 mm (ground target), 13.3 mm (Starlette), and 16.9 mm (Lageos). The precisions of the best performing ranging targets are 1.1 mm, 2.5 mm, and 3.0 mm, whereas the worst are 39.3 mm, 28.7 mm, and 31.8 mm. However, the single-shot precision of the Geochang SLR system is 3.6 mm (ground target), 5.3 mm (Starlette), and 7.1 mm (Lageos-2), which is better than the average values of the ILRS tracking stations.

4. CONCLUSIONS

The Korea Astronomy and Space Science Institute has been developing the SOLT system, which comprises SLR, AO, and DLT systems, at the Geochang station for space geodesy, SSA, and Korean space missions. The three systems share numerous subsystems, such as the optical telescope and tracking mount, because they have the same optical path from the primary mirror to the switching mirror. It is designed to be capable of laser ranging up to GEO satellites with an LRA, space objects imaging brighter than magnitude 10, and laser tracking to LEO space debris without an LRA. These systems are operated independently, not simultaneously, by employing a switching mirror feeding the beam path to each system. The SLR and AO systems have been established at the Geochang station, whereas the DLT system is currently under development and the AO system is being prepared for testing.

The design and development of the SOLT system were addressed in this study and the representative observations of the SLR system were both discussed and analyzed for the performance evaluation. The SLR data quality of the ILRS tracking station was evaluated in terms of single-shot precision for the ground target, and Starlette and Lageos

satellites. The single-shot precision of the Geochang SLR system was 3.6 mm for the ground target, 5.3 mm for the Starlette satellite, and 7.1 mm for the Lageos-2 satellite, which was better than the mean values of the ILRS tracking stations. In addition, it was shown that the SLR system is capable of laser ranging up to GEO satellites, including the GNSS satellites. Because of the tracking capability and ranging performance, the SLR system will not only play an important role as a member of the ILRS tracking network, but also contribute to future Korean space missions, such as the Korean navigation system and Korean GEO satellites. In addition, it is expected that, after development of the AO and DLT systems, the SOLT system will become an essential ground station for SSA applications.

ACKNOWLEDGMENTS

This study was supported by the Korea Astronomy and Space Science Institute through “Operation and Research for Satellite Laser Ranging System” project funded by the Ministry of Science and ICT (MSIT) of the Korean government.

REFERENCES

Bennet F, Price I, Rigaut F, Copeland M, Satellite imaging with adaptive optics on a 1 m telescope, in 17th Advanced Maui Optical and Space Surveillance Technologies (AMOS) Conference, Maui, Hawaii, USA, 20-23 Sep 2016.

Bennett JC, Sang J, Smith C, Zhang K, An analysis of very short-arc orbit determination for low-Earth objects using sparse optical and laser tracking data, *Adv. Space Res.* 55, 617-629 (2015). <https://doi.org/10.1016/j.asr.2014.10.020>

Choi EJ, Bang SC, Sung KP, Lim HC, Jung CG, et al., Design and development of high-repetition-rate satellite laser ranging system, *J. Astron. Space Sci.* 32, 209-219 (2015). <https://doi.org/10.5140/jass.2015.32.3.209>

Choi MS, Lim HC, Choi EJ, Park E, Yu SY, et al., Performance analysis of the first Korean satellite laser ranging system, *J. Astron. Space Sci.* 31, 225-233 (2014). <https://doi.org/10.5140/jass.2014.31.3.225>

- org/10.5140/jass.2014.31.3.225
- Gebhardt FG, High power laser propagation, *Appl. Opt.* 15, 479-2493 (1976). <https://doi.org/10.1364/AO.15.001479>
- Greene B, Gao Y, Moore C, Wang Y, Boiko A, et al., Laser tracking of space debris, *Proceedings of 13th International Laser Ranging Workshop*, Washington D.C., USA, 7-11 Oct 2002.
- Grosse D, Bennet F, Copeland M, d'Orgeville C, Rigaut F, et al., Adaptive optics for satellite imaging and Earth based space debris manoeuvres, *Proceedings of 7th European Conference on Space Debris*, Darmstadt, Germany, 18-21 Apr 2017.
- Hampf D, Wagner P, Riede W, Optical Technologies for observation of low Earth orbit objects, in *65th International Astronautical (IAC) Congress*, Toronto, Canada, 29 Sep - 3 Oct 2014.
- ILRS, International Laser Ranging Service website [Internet], cited 2018 Nov 27, available from: <https://ilrs.cddis.eosdis.nasa.gov>
- Kessler DJ, Cour-Palais BG, Collision frequency of artificial satellites: the creation of a debris belt, *J. Geophys. Res.* 38, 2637-2646 (1978). <https://doi.org/10.1029/JA083iA06p02637>
- Kirchner G, Koidl F, Friederich F, Buske I, Volker U, et al., Laser measurements to space debris from Graz SLR station, *Adv. Space Res.* 51, 21-24 (2013). <https://doi.org/10.1016/j.asr.2012.08.009>
- Lejba P, Suchodolski T, Michalek P, Bartoszak J, Schillak S, et al., First laser measurements to space debris in Poland, *Adv. Space Res.* 61, 2609-2616 (2018). <https://doi.org/10.1016/j.asr.2018.02.033>
- Lim HC, Bang SC, Yu SY, Seo YK, Park E, et al., Study on the Optoelectronic design for Korean mobile satellite laser ranging system, *J. Astron. Space Sci.* 28, 155-162 (2011). <https://doi.org/10.5140/jass.2011.28.2.155>
- Liou J, Engineering and technology challenges for active debris removal, *Prog. Propuls. Phys.* 4, 735-748 (2013). <https://doi.org/10.1051/eucass/201304735>
- Mason J, Stupl J, Marshall W, Levit C, Orbital debris-debris collision avoidance, *Adv. Space Res.* 48, 1643-1655 (2011). <https://doi.org/10.1016/j.asr.2011.08.005>
- Oh H, Park E, Lim HC, Lee SR, Choi JD, et al., Orbit determination of high-Earth-orbit satellites by satellite laser ranging, *J. Astron. Space Sci.* 34, 271-280 (2017). <https://doi.org/10.5140/JASS.2017.34.4.271>
- Urschl C, Gurtner W, Hugentobler U, Schaer S, Beutler G, Validation of GNSS orbits using SLR observations, *Adv. Space Res.* 36, 412-417 (2005). <https://doi.org/10.1016/j.asr.2005.03.021>
- Zhang ZP, Yang FM, Zhang HF, Wu ZB, Chen JP, et al., The use of laser ranging to measure space debris, *Res. Astron. Astrophys.* 12, 212-218 (2012). <https://doi.org/10.1088/1674-4527/12/2/009>
- Zovaro A, Bennet F, Copeland M, Rigaut F, d'Orgeville C, et al., Harnessing adaptive optics for space debris collision mitigation, in *17th Advanced Maui Optical and Space Surveillance Technologies (AMOS) Conference*. Maui, Hawaii, USA, 20-23 Sep 2016.

